Effects of chlorine and oxygen coverage on the structure of the Au(111) surface

Thomas A. Baker,[1] Cynthia M. Friend,[1,2] and Efthimios Kaxiras[1,2,3,a)]
[1]*Department of Chemistry and Chemical Biology, Harvard University, 12 Oxford Street, Cambridge, Massachusetts 02138, USA*
[2]*School of Engineering and Applied Sciences, Harvard University, Cambridge, Massachusetts 02138, USA*
[3]*Department of Physics, Harvard University, 17 Oxford Street, Cambridge, Massachusetts 02139, USA*

(Received 4 October 2008; accepted 23 December 2008; published online 23 February 2009)

We investigate the effects of Cl and O coverage on the atomic structure of the Au(111) surface using density functional theory calculations. We find that the release and incorporation of gold atoms in the adsorbate layer becomes energetically favorable only at high coverages of either O or Cl (>0.66 ML (monolayer) for O and >0.33 ML for Cl), whereas adsorption without the incorporation of gold is favorable at lower coverages. The bonding between the adsorbate and gold substrate changes significantly with coverage, becoming more covalent (less ionic) at higher Cl and O coverage. This is based on the fact that at higher coverages there is less ionic charge transfer to the adsorbate, while the electron density in the region between the adsorbate and a surface gold atom is increased. Our results illustrate that the O and Cl coverage on Au(111) can dramatically affect its structure and bonding, which are important features in any application of gold involving these adsorbates. © *2009 American Institute of Physics*. [DOI: 10.1063/1.3077314]

I. INTRODUCTION

Gold surfaces play a vital role in all aspects of modern technology and science, from heterogeneous catalysis to nanotechnology.[1] Gold is extensively used as a substrate for self-assembled monolayers[2,3] in materials science,[4] as interconnects in electronic devices,[5–7] as a substrate for conducting polymers in chemical sensors,[8] and in many different types of biosensors.[9,10] Gold can be used in plasmonic electronic devices and is an important substrate for surface enhanced Raman spectroscopy.[11,12] Since such applications rely on some of the unique electronic features of gold, a complete understanding of the gold surface as well as the bonding of adsorbates on gold surfaces is crucial.

The surface morphology of gold can have a significant role in determining its properties. For example, the size[13,14] and shape[15] of a supported Au nanoparticle has a substantial effect on its catalytic activity: smaller particles (2–4 nm in diameter) have much greater catalytic activity than larger ones (20–40 nm in diameter), with rate constants differing by as much as two orders of magnitude.[16] On the surface of gold, the adsorption of electronegative species has been found to affect significantly the morphology of the surface. Adsorbates including NO_2,[17] S,[18] and CH_3SH (Refs. 19 and 20) can lift gold atoms from the surface. Au(111) may be especially prone to the release of gold atoms due to the "herringbone" reconstruction which contains an excess of ~4.5% Au atoms compared to the bulk (111) plane, with some of these extra atoms weakly bound at "elbow" sites.[21–23] The presence of adsorbed molecules can lift the herringbone structure, releasing gold adatoms on the surface.[24–26] The adsorption of atomic oxygen creates small gold islands on the surface[27] which are formed because oxygen can stabilize undercoordinated Au.[28] The morphology of these islands can also affect the reactivity of the surface.[29] Atomic chlorine also releases gold on Au(111), a process which is dynamical in nature and involves many different structures and types of Cl bonding to Au.[30,31] Depending on Cl coverage, the surface can exhibit initial release of gold atoms from the herringbone reconstruction, a chemisorbed overlayer, and further release of gold atoms to form a gold chloride layer.[32]

In the present work, we study these phenomena which are important for understanding the catalytic properties of the gold surface, using first-principles electronic structure calculations based on density functional theory (DFT). We investigate the energetics of the morphological change of the Au(111) surface upon the adsorption of two different electronegative species, chlorine and oxygen. By examining the electronic charge density and the density of states (DOS) we provide insight into the physical origin of our results, which elucidate recent experimental observations on these systems.

The paper is organized as follows: Sec. II describes the DFT calculations employed in our work. Section III describes the effect of coverage and gold adatom incorporation on the total energy for adsorption of Cl and O on Au(111), along with the effect of the oxygen chemical potential on the surface free energy. Section IV discusses the observed trends and impacts on bonding by investigating the electronic charge density and DOS for Cl adsorption, followed by Sec. V, the conclusions.

a)Author to whom correspondence should be addressed. Also at Lyman Laboratory, 17 Oxford Street, Cambridge, MA 02138. Tel.: 617-495-7977. FAX: 617-496-2545. Electronic mail: kaxiras@physics.harvard.edu.

II. CALCULATIONAL DETAILS

The DFT results were preformed with the VASP code[33] using the GGA-PW91 functional[34] to model electron exchange and correlation. Ultrasoft pseudopotentials were used with the default plane-wave cutoffs for different elements taken from the generalized gradient approximation (GGA) ultrasoft-pseudopotential database.[35,36] We use a 12 layer slab and a $(\sqrt{3}\times\sqrt{3})R30°$ surface unit cell to model the Au(111) surface, with the bottom six layers remaining fixed in their bulk positions and the top six layers allowed to relax. The surface supercell does not capture the herringbone reconstruction, which we expect to not have important effects on the energetics, and which is typically lifted upon adsorption of foreign atoms. The clean Au(111) surface corresponds to a bulk terminated plane. A large vacuum region between the slabs of ~20 Å was used to ensure that the dipole induced by the presence of adsorbates on one side of the slab does not create artifacts due to interaction between neighboring unit cells. A Monkhorst–Pack Γ-centered $6\times6\times1$ k-point scheme was used for reciprocal-space sampling. We find that spin polarization has no significant effect on the total energy comparisons.

Our choice of the PW91 exchange-correlation functional, instead of functionals such as Perdew-Burke-Ernzerhof (PBE) and revised-PBE (RPBE), was based on the fact that it provides a better description of Au–Au binding, which is important in addressing the differences in energy between a clean and an adatom-covered gold surface. In general, DFT-GGA calculations underestimate the cohesive energy of metals. We find that the underestimation is most extreme with the RPBE functional: the calculated cohesive energy, using the PW91, PBE, and RPBE functionals are −3.02, −2.99, and −2.38 eV, while the experimental value is −3.81 eV.[37] The same trend was found for the surface energy, calculated using the PW91, PBE, and RPBE functionals: 0.0437, 0.0381, and 0.0153 eV/Å^2, respectively, versus the experimental value of 0.0936 eV/Å^2.[38] Since the PBE and RPBE functionals greatly underestimate the cohesive energy and surface energy, they are likely to give less accurate results for the cost of creating a gold atom or vacancy, compared to the PW91 functional. We provide an estimate of the error introduced by our choice of functional by using different functionals to obtain the relative energies for important structures and assigning the difference in these energies as the uncertainty of the calculation (see Sec. III and the discussion related to Fig. 3).

In order to provide insight into the physical origin of the results, we calculated the charge associated with specific atoms in selected configurations. There are different approaches to calculating the charge of atoms when using a plane-wave basis, most of them involving integration of the charge in a volume centered at the nucleus of the atom. We used two different methods for integrating the electronic charge: the first method consists of using spheres to integrate the amount of charge around an atom, which is a convenient and physically reasonable approximation. The radius of the sphere is determined by the distance of the minimum value of the electron density between the adsorbate and the nearest surface Au atom. The difference between the integrated density in the adsorbed system and a free adsorbate atom in the gas phase is defined as the net charge. The second method, suggested by Bader,[39] is similar, but more mathematically rigorous: instead of using atom-centered spheres, the density is partitioned into nonoverlapping basins defined by surfaces on which the electron density gradient vanishes.[40] There are small differences in the charge calculated from the two methods, but the qualitative trends that emerge are the same.

III. RESULTS

The first system we considered is the adsorption of 0.33 and 0.67 ML (monolayer) of Cl on Au(111). The adsorption energy for p chlorine atoms is defined relative to the Cl_2 reservoir,

$$E_{\text{Cl-ads}}(p) = E_{\text{Au/Cl}} - E_s - \frac{p}{2}E_{\text{Cl}_2}, \tag{1}$$

where $E_{\text{Au/Cl}}$ is the total energy of the system consisting of the Au surface with p Cl atoms bound on the gold substrate, E_s is the energy of the gold substrate, and E_{Cl_2} is the energy of the Cl_2 molecule The calculated bond length and binding energy for Cl_2 using the PW91 functional is 2.02 Å and 2.68 eV, respectively, which compares well with the experimental values of 1.99 Å and 2.48 eV.[41] With a different exchange-correlation functional [RPBE (Ref. 42)], these values are 2.00 Å and 2.54 eV.[43]

Experimentally, gold atoms are only incorporated in the adsorbate structure at Cl coverages above 0.33 ML.[32] In order to investigate the energetics for gold incorporation as a function of Cl coverage, we considered the adsorption of chlorine on three different Au(111) substrates: a clean surface and surfaces covered with 0.33 and 0.67 ML of Au adatoms. It is important to note that at Cl coverages above 0.33 ML, a wide variety of periodic and aperiodic structures were observed experimentally with scanning tunneling microscopy (STM).[32] The exact stoichiometry and unit cell dimensions along with clear atomic resolution of the structures could not be determined from these STM studies. Since we are interested in understanding gold incorporation as a function of coverage and not the exact structure at higher coverages, we use the $(\sqrt{3}\times\sqrt{3})R30°$ unit cell as a model for all Cl coverages. We expect that factors such as adsorbate-adsorbate repulsion that lead to Au incorporation will be qualitatively similar in the real and model systems, thus our model can provide insight into the coverage-dependent bonding of adsorbates on the gold surface.

To compare the adsorption of chlorine on each substrate, the total energy is calculated as

$$E_{\text{tot}}(n,p) = E_{\text{Cl-ads}}(p) + E_{\text{cost}}(n), \tag{2}$$

where $E_{\text{cost}}(n)$ is the energy cost for creating n gold adatoms,

$$E_{\text{cost}}(n) = E_{s\text{-ad}}(n) - nE_b - E_s, \tag{3}$$

with $E_{s\text{-ad}}(n)$ as the total energy of the Au(111) substrate with n adatoms, E_b the energy of a gold atom in the bulk, and E_s, in this case, the energy of the bare Au(111) substrate. This energy cost was calculated for coverages corresponding to

TABLE I. Summary of total energies, $E_{tot}(n,p)$, defined in Eq. (2), for two Cl coverages, p [expressed in ML for the $(\sqrt{3}\times\sqrt{3})R30°$ unit cell] on Au(111) with different gold adatom coverages, n. Bold characters indicate the systems with the lowest energy at each chlorine and adatom coverage.

	p (ML)			
	0.33 ML Cl		0.67 ML Cl	
n (ML)	Site	E_{tot} (eV)	Site	E_{tot} (eV)
0.00	Top	−0.65	Bridge	−0.37
	Bridge	−0.87		
	hcp	−0.88		
	fcc	−0.91		
0.33	Top	−0.43	$AuCl_2$	−0.54
	Side	−0.47		
0.67	Bridge	−0.81	Half bridge	−0.57
	Hollow	−0.24	Top	−0.20

0.33 ML [$n=1$ in the $(\sqrt{3}\times\sqrt{3})R30°$ unit cell] and 0.67 ML [$n=2$] of adatoms on the top layer and found to be 0.75 and 0.65 eV, respectively. The cohesive energy of bulk Au is −3.02 eV, the Au–Au dimer cohesion is −2.24 eV, and the Au–Cl pair cohesion is −2.91 eV. Adatom formation and incorporation into a chloride layer can only take place if

$$E_{\text{Cl-ads}}(p) - E_{tot}(n,p) > 0, \tag{4}$$

where $E_{\text{Cl-ads}}(p)$ is the lowest adsorption energy possible for chlorine bound on the clean adatom-free surface and $E_{tot}(n,p)$ is the lowest energy for chlorine on an adatom-covered surface.

The energetics of 0.33 ML Cl adsorption on a $(\sqrt{3}\times\sqrt{3})R30°$ unit cell on the three different types of substrates of Au(111) was studied in previous work.[32] To summarize those results, the system with the lowest energy consists of Cl binding in fcc threefold sites on the clean surface with an adsorption energy of −0.91 eV (Table I). The adsorption of Cl on adatom-covered Au(111) surfaces was stronger, but not enough to compensate for the cost to create the adatom surface, $E_{cost}(n)$.

By taking into account the cost required to create each surface, it is possible to determine the adsorption species with the lowest energy for the adsorption of 0.67 ML of Cl. The first system we considered is the adsorption of chlorine on the clean adatom-free surface. We find that chlorine binds preferentially on bridge sites, forming a honeycomb pattern on the surface, Fig. 1(a), with an adsorption energy of −0.18 eV per Cl and a Cl–Au distance of 2.60 Å. The repulsive interaction between neighboring chlorine atoms at a Cl coverage of 0.67 ML weakens the Au–Cl interaction in comparison to the case of 0.33 ML coverage. In the latter case, Cl adsorption prefers a higher coordination to gold (the fcc threefold site), has a lower adsorption energy (−0.91 eV per Cl), and a slightly smaller Au–Cl length, 2.58 Å.

We also considered the adsorption energy of chlorine on a surface containing 0.33 ML of gold adatoms. We find that chlorine binds much more strongly to this surface compared to the flat adatom-free surface. The lowest energy configuration has two chlorine atoms bound on top of a gold adatom, on either side and coordinated only to the gold adatom, Fig. 1(b). The adsorption energy for this structure is −0.64 eV per Cl, significantly lower than for the 0.67 ML Cl coverage on the clean surface. In fact, the adsorption energy is sufficiently lowered to compensate for the cost of creating the Au adatoms, resulting in a surface that is lower in total energy (Table I).

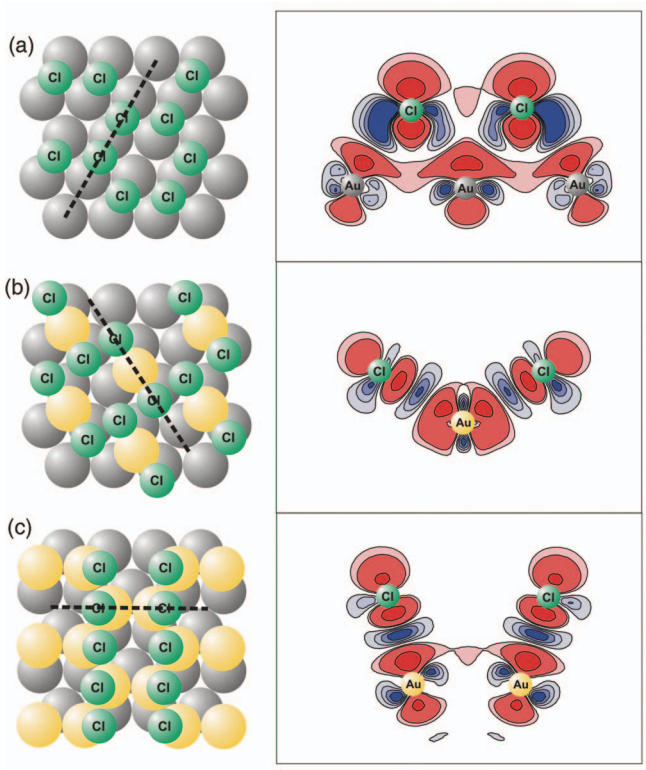

FIG. 1. (Color) Lowest-energy structures (left panels) and charge density difference plots (right panels) of 0.67 ML Cl adsorption on: (a) flat (1×1) surface; (b) Au(111) covered with 0.33 ML Au adatoms; (c) 0.67 ML Au adatoms. The darker gray circles represent the top full layer of gold atoms, lighter yellow circles represent gold adatoms, and small (green) circles represent chlorine atoms. The thick dotted lines on the structural figures on the left show the planes on which the density difference is plotted. Red contours correspond to charge depletion and blue contours to charge accumulation.

The last structure we considered is chlorine adsorbed on 0.67 ML of gold adatoms (equivalent to 0.33 ML of gold vacancies). In this case, the preferred binding site for chlorine is on a "half-bridge site" on the gold atoms that make up the top layer of the surface, Fig. 1(c): in this configuration, Cl is bound directly to one gold atom but in an off-center position, tilted towards the vacancy and close to what would have been the bridge site of the surface without the vacancy. An alternative structure, with the Cl atom directly on top of the gold atom is substantially higher in energy (Table I). The binding energy for chlorine on the half-bridge site is −0.61 eV per Cl. As in the case of chlorine adsorption on the 0.33 ML adatom-covered surface, the Au–Cl interaction is much stronger and the Au–Cl length is smaller for a surface that contains 0.67 ML adatoms compared to the clean Au(111) surface. The Au–Cl length is 2.60 Å for Cl on a flat surface, but only 2.46 Å on the 0.67 ML adatom-covered surface. When taking into account the cost of creating the adatom-

TABLE II. Summary of total energies, $E_{tot}(n,p)$ for three O coverages, p, on Au(111) with different gold adatom coverages, n. Notation is the same as in Table I. Energies in brackets are from the PBE functional and are used to estimate the error in Fig. 3.

	p (ML)					
	0.33 ML O		0.67 ML O		1.00 ML O	
n (ML)	Site	E_{tot} (eV)	Site	E_{tot} (eV)	Site	E_{tot} (eV)
0.00	fcc	0.16[0.16]	fcc	1.13[1.10]	Bridge	3.45[3.45]
0.33	Top Side	1.73 1.86	Flat AuO_2	1.50[1.47]	Trigonal Pyramid	2.64[2.61]
0.67	Half bridge	0.73[0.67]	Half bridge	1.85		

covered surface, chlorine bound at half-bridge sites on the 0.67 ML adatom-covered surface is the lowest energy structure (Table I).

To illustrate that the results above are not just characteristic of the chlorine-gold interaction, but rather they apply generally to electronegative atoms on gold, the same substrates were used to study oxygen adsorption at different coverages. We find that at a coverage of 0.33 ML, oxygen prefers to bind in a fcc threefold site with an adsorption energy of 0.18 eV. This agrees well with previously published results: an adsorption energy of 0.16 eV was reported using the PW91 functional for an oxygen coverage of 0.25 ML.[44] The adsorption energy can also be defined relative to an oxygen atom instead of an oxygen molecule; using this definition Gajdos *et al.*[45] reported an adsorption energy of −2.95 eV for a coverage of 0.25 ML, while we find this energy to be −2.84 eV. The overlayer on the clean (adatom-free) surface is the lowest energy structure for 0.33 ML coverage of oxygen (Table II), as was the case for chlorine. The Au–O dimer cohesion energy is −2.57 eV. On the 0.33 ML adatom-covered surface, in contrast to the chlorine adsorption, the adsorption of oxygen is not stronger compared to the adatom-free surface for 0.33 ML of oxygen. Adsorption on the 0.67 ML adatom-covered surface was slightly stronger (by 0.08 eV) than on the (1×1) clean surface, but this difference is not enough to compensate for the cost of creating the adatoms on the surface.

For 0.67 ML coverage of oxygen, the most stable structure is still the oxygen overlayer without gold incorporation, Fig. 2(a). Due to the repulsion of neighboring oxygen atoms, the 0.67 ML overlayer structure has a higher adsorption energy (0.56 eV per O) compared to the 0.33 ML overlayer (0.16 eV per O). For oxygen adsorption on the 0.33 ML adatom-covered surface, the structure with the lowest energy consists of oxygen bound on either side of the gold adatom, coordinated to both the adatom and the top complete layer of gold atoms, Fig. 2(b). The adsorption energy for this structure is 0.18 eV per O lower than the overlayer, but this difference is not enough to make up for the energy cost of creating the gold adatoms on the surface. The structure with the lowest energy on the 0.67 ML adatom-covered surface has two oxygen atoms bound off-center from the adatom and interacting with the vacancy below; however, this system is 0.72 eV higher in energy than the overlayer.

At a coverage of 1.00 ML of oxygen, adatom incorporation becomes energetically favored over formation of the overlayer. The preferred binding site for the 1.00 ML overlayer structure is oxygen on bridge sites, with an adsorption energy of 1.15 eV per O. The 0.33 ML adatom-covered gold surface, however, has an adsorption energy of 0.63 eV per O, which is significantly lower than the overlayer and can easily compensate for the cost of creating the adatom. In this structure, the gold adatom sits on a threefold site with each oxygen in the plane of the gold adatom and coordinated to both the adatom and the top gold layer, Fig. 2(c).

Experimentally, atomic oxygen is often introduced to gold using various methods including electron bombardment

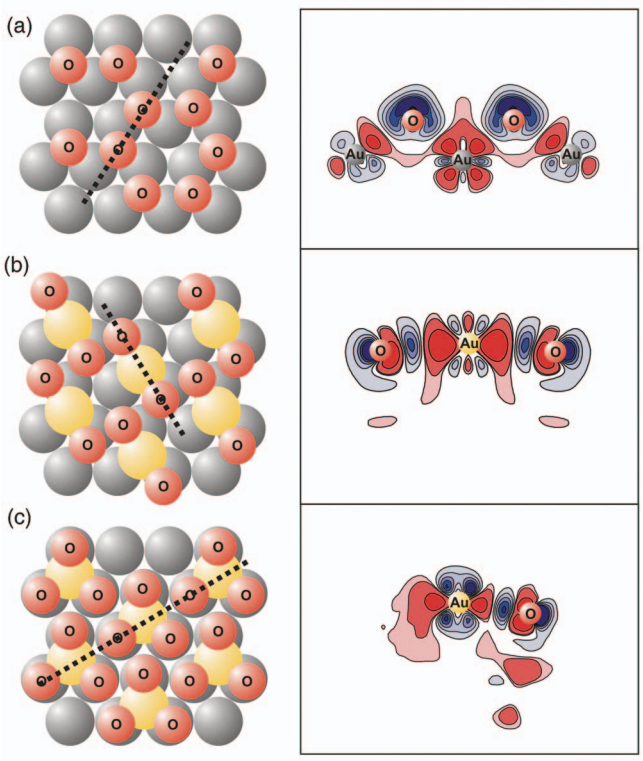

FIG. 2. (Color) Lowest-energy structures (left panels) and charge density difference plots (right panels) of: (a) 0.67 ML O adsorption on flat, (1×1) Au(111) surface; (b) 0.67 ML O adsorption on Au(111) surface covered with 0.33 ML adatoms; (c) 1.00 ML O adsorption on 0.33 ML Au adatom-covered Au(111) surface. Symbols are the same as in Fig. 1, with red for O atoms.

of condensed NO_2,[46] ion sputtering with O_2,[47,48] thermal dissociation of gaseous O_2 using hot filaments,[49] and exposure to ozone.[50] Since the source of oxygen in these experimental results is not necessarily oxygen gas but a variety of sources, it is useful to consider the phase diagram of surface free energy as a function of the oxygen chemical potential.

We start with the assumption that the surface is in thermodynamic equilibrium with the separate reference phases at a given temperature T and pressure P. The environment acts as a reservoir where oxygen can adsorb or desorb from the surface without a change in pressure or temperature. The Gibbs free energy $G(T,P,N_{Au},N_O)$ is the thermodynamic potential required to describe this system. The most stable surface minimizes the surface free energy, $\gamma(T,P)$, defined as

$$\gamma(T,p) = (1/A)[G(T,P,N_{Au},N_O) - N_{Au}\mu_{Au}(T,P) - N_O\mu_O(T,P)], \quad (5)$$

where μ_{Au} and μ_O are the chemical potentials of a Au atom and an O atom, N_{Au} and N_O are the numbers of these species, and the surface energy has been normalized by dividing by the surface area, A.[51–53] In principle, the Gibbs free energy could be calculated by considering the contributions of vibrational and configurational entropy; in practice these contributions are small and can be neglected allowing the terms to be approximated as DFT total energies.[54] The surface free energy becomes

$$\gamma_{DFT}(T,P) = (1/A)[E(\mathrm{Au/O}) - E(\mathrm{Au}) - N_O\mu_O(T,P)], \quad (6)$$

where $E(\mathrm{Au/O})$ is the total energy of the system consisting of the Au surface with O atoms bound on the surface and $E(\mathrm{Au})$ is the energy of the gold substrate. The chemical potential of oxygen could be related to an oxygen pressure and temperature by calculating the translational and rotational partition functions of the gas phase, but for a qualitative phase diagram it suffices to consider the upper and lower bound of the chemical potential.[51] The lowest possible bound of the oxygen chemical potential, which would correspond to an infinitely small pressure of oxygen, is equal to the cost of forming an atomic oxygen atom from the reference reservoir of the molecular solid: $[E(O_{2(s)}) - 2E(O)]/2$, which is also the bond dissociation energy per oxygen atom. A more realistic lower bound is the bond dissociation energy per oxygen atom from oxygen gas. Adsorbing oxygen on the surface at no cost ($\mu_O = 0$) represents the upper bound (high oxygen pressure), therefore the range in chemical potential is

$$-3.0 \text{ eV} < \mu_O < 0, \quad (7)$$

where for consistency in the theoretical results[51] we use the value of $[E(O_{2(g)}) - 2E(O)]/2 \approx -3.0$ eV obtained from our calculations. Figure 3 is a plot of the surface free energy as a function of oxygen chemical potential between the two extreme bounds. Oxygen dissociation is not thermodynamically favorable in the small unlabeled region in Fig. 3 close to the lower bound of the chemical potential. As the oxygen chemical potential increases, a higher oxygen coverage is possible on the surface creating three distinct regions, labeled Ia, Ib, and II in Fig. 3. The possible error in the calculation due to the choice of exchange-correlation functional is illustrated as a range of values in the chemical potential for the transition between different regions; this was estimated by using two different functionals (PW91 and PBE) to obtain the energy versus chemical potential curves. The structures with the lowest surface free energy in regions Ia and Ib are the 0.33 and 0.67 ML of oxygen coverage without gold adatom incorporation, respectively. The transition between a flat surface and gold incorporation occurs between regions I and II when the oxygen coverage with the lowest energy increases from 0.67 to 1.00 ML.

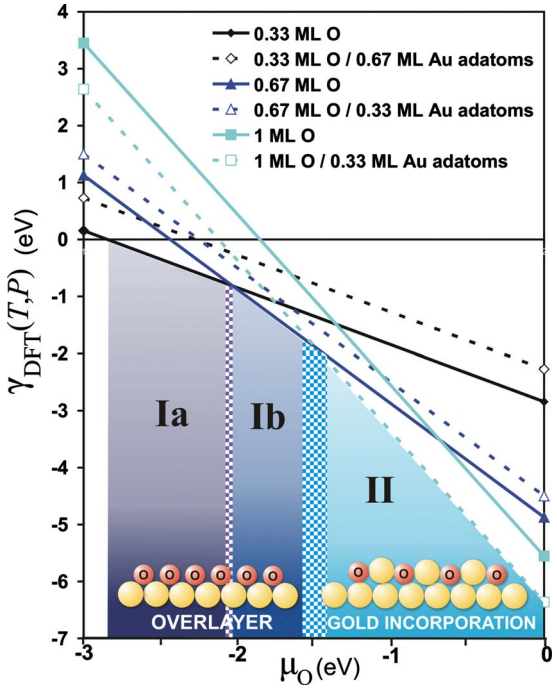

FIG. 3. (Color online) Surface free energy $\gamma_{DFT}(T,P)$ as a function of the oxygen chemical potential μ_O for different oxygen and gold adatom coverages. The clean surface is represented by a horizontal line at a surface free energy of 0 eV. The transition range in the oxygen chemical potential between regions, representing the error introduced by the choice of exchange-correlation functional, is indicated by checkered-square region.

The surface free energy plot is consistent with the experimental observation that the adsorption of ozone in ultrahigh vacuum on the Au(111) surface always results in gold adatoms being released, regardless of oxygen coverage.[27] The experimental chemical potiental,[55] -1.05 eV, lies well within region II, where gold adatom incorporation is favorable. This also agrees with Shi and Stampfl[56] who recently preformed similar calculations using a larger unit cell; they predict that the energetically most favorable configuration is a "surface-oxide-like" layer that has gold incorporated in its structure.

IV. DISCUSSION

Our results show that the incorporation of Au into an adsorbate layer depends on the coverage of the electronegative atom. At low coverages, Au adatom or vacancy formation is not favorable, while at high coverages defect formation becomes energetically favorable. In general, the adsorbate binds more strongly to a surface containing defects, but the gain in energy due to the stronger binding to

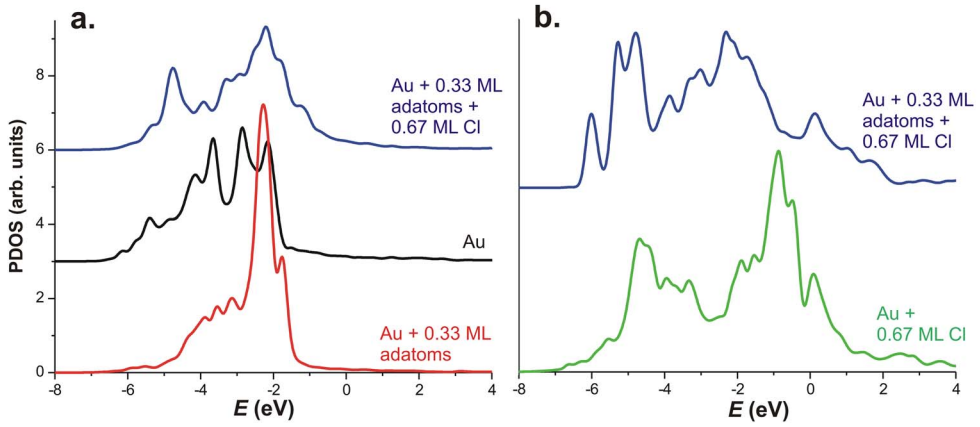

FIG. 4. (Color online) (a) Au *d*-PDOS vs energy *E* for the surface gold atom of the clean surface, gold adatom for the 0.33 ML adatom-covered surface, and gold adatom for the 0.33 ML adatom-covered surface with 0.67 ML Cl. (b) Cl *p*-PDOS vs energy *E* for 0.67 ML of chlorine on the clean surface and 0.33 ML Au adatom-covered surface. The zero of the energy scale is the Fermi level.

the surface does not compensate for the cost of creating the defected surface at low adsorbate coverages. The energy gained from adsorption to a defect-containing surface increases with increasing coverage, which leads to a transition when the energy cost of defect formation can be overcome. This gain in energy at higher coverages is not just the result of adding adsorbate atoms, but rather due to the fact that the gold-adsorbate interaction changes with increasing coverage. To illustrate, at 0.33 ML of chlorine coverage the difference between the adsorption of Cl on a clean surface and on 0.67 ML adatom-covered surface is −0.31 eV per Cl. At 0.67 ML chlorine coverage, a second chlorine atom is added to the $(\sqrt{3}\times\sqrt{3})R30°$ unit cell, but the difference in the total binding energy between chlorine on the flat surface and the 0.67 ML adatom-covered surface is not simply twice the difference at 0.33 ML (−0.62 eV), but larger (−0.86 eV) and adequate to compensate for the cost of creating the adatom surface (0.65 eV). To account for this effect, there must be differences in the bonding of the adsorbate at different coverages. In the following discussion, we will analyze the DOS to identify specifically which states are affected by gold incorporation, and consider charge density plots in an attempt to understand the bonding differences for chlorine at different coverages.

Partial density of states (PDOS) plots provide insight into the ability of chlorine to stabilize adatoms on the gold surface. A comparison of the Au *d*-PDOS for the Au(111)-(1×1), the surface containing 0.33 ML of adatoms, and the adatom-covered surface with 0.67 ML Cl, provides insight into bonding changes, Fig. 4(a). As expected, without chlorine adsorbed on the surface, the Au *d* states are higher in energy for the gold adatoms, suggesting that these adatoms are more reactive.[57,58] With chlorine adsorbed, the gold adatom *d* electronic states are significantly lowered in energy, suggesting that adsorbed Cl can stabilize adatoms that are created on the surface. This explains why the adsorption energy for chlorine on adatoms at any coverage is lower than for overlay adsorption.

The *p*-PDOS for 0.67 ML Cl on the clean and adatom-covered surfaces indicates that the adsorption of Cl on the adatom-covered surface lowers the energy of Cl since the *p*-PDOS is generally lower in this case, Fig. 4(b). The same trend is observed for the *s* states of Cl and could explain why the neighboring Cl–Cl distance is smaller on the adatom-covered surface: 2.92 Å on the clean surface versus 2.57 Å on the adatom-covered surface.

Charge density plots of Cl and O on various gold substrates illustrate that the Cl–Au and O–Au bonds become more covalent with gold incorporation. Figure 1 shows the charge density difference plots for 0.67 ML of Cl on (a) the clean gold surface, (b) the 0.33 ML Au adatom-covered surface, and (c) the 0.67 ML Au adatom-covered surface. The charge density differences are defined as the electron density of the total adsorbed system minus the density of just the Au substrate and Cl atom in the exactly same positions as in the adsorbed system. As mentioned earlier, the overlayer (a) is the highest in energy followed by the 0.33 ML adatom-covered surface (b), with the 0.67 ML adatom-covered surface being the most stable. The charge difference plots illustrate the bonding between Cl and Au on these three surfaces. In previous work, we found that the Cl–Au interaction on the Au(111) surface is mainly covalent in nature.[59] The same is true for these three systems, only in the case of gold incorporation the chlorine atom forms an even stronger covalent bond with the gold substrate. Figures 1(b) and 1(c) illustrate the accumulation of electron density directly between Cl and Au. The electron density minimum on the line connecting the Cl and Au positions increases as the energy of the system decreases. The density minimum for the clean, 0.33 ML Au adatom covered, and 0.67 ML Au adatom-covered surface for 0.67 ML of Cl is 0.38, 0.45, and 0.51, respectively. The Au–Cl bond distance follows the same trend, namely, 2.60, 2.51, and 2.46 Å, respectively.

The same trend is also observed for oxygen: as the overlayer coverage increases from 0.33 to 0.67, to 1.00 ML the minimum value of the charge density increases from 0.59 to 0.67, to 0.82 respectively. The system with the lowest energy for 1.00 ML of oxygen contains 0.33 ML of gold adatoms; this O–Au bond has the highest amount of electron density directly along the bond, 1.10. As the coverage increases, the

TABLE III. Summary of calculated charges for different coverages of O and Cl (p) on Au(111) with different gold adatom coverages (n). The two different methods of calculating charge are indicated, (A) sphere, or (B) Bader method.

	p (ML)					
	0.33 ML Cl		0.67 ML Cl			
n (ML)	A	B	A	B		
0.00	−0.33	−0.37	−0.33	−0.28		
0.33	−0.20	−0.41	−0.27	−0.20		
	0.33 ML O		0.67 ML O		1.00 ML O	
	A	B	A	B	A	B
0.00	−0.54	−0.77	−0.56	−0.70	−0.40	−0.58
0.33	−0.40	−0.59				

number of gold atoms to which the adsorbate is coordinated decreases. The charge density difference plots (Fig. 2) illustrate that more electron density is added directly between the adsorbate and gold adatom with increasing coverage, suggesting a stronger covalent interaction similar to the trend observed for Cl. There are some important differences, however, between the Cl and O charge density difference plots. For oxygen adsorption on the adatom-covered surfaces, electron density is added both between the O and Au adatom and on the back side of O, while for Cl electron density is only added directly between Cl and the Au adatom. The electron density accumulation on the back side of the O atom (opposite of the adatom) is attributed to the oxygen binding much closer to the surface than Cl, preferring higher coordination to Au compared to Cl; this results in bonding not just between oxygen and the adatom, as in the Cl case, but also between O and the underlying gold in the first complete layer.

The charge on the adsorbate also provides evidence that the bonding becomes more covalent with gold incorporation or at higher adsorbate coverages. Table III contains the charge, calculated using both the sphere and Bader method, for various adsorption systems. The charge changes significantly as a function of the coverage and gold incorporation. Generally, as the coverage of the adsorbate increases or if gold is incorporated into the adsorbate layer, the magnitude of the negative charge decreases. For example, as the oxygen overlayer coverage increases, the charge from the Bader method decreases from −0.77 at 0.33 ML to −0.58 at 1.00 ML. The same is observed for Cl and at the same Cl coverage, gold incorporation lowers the charge. The smaller partial negative charge on the adsorbate may occur partly because the adsorbate is coordinated to fewer gold atoms and these gold atoms have more than one electronegative atom bound to them so that a smaller amount of electron density is available to be pulled by the adsorbate atom. These results combined with the charge density plots indicate that the smaller negative charge is also a result of the increased covalent nature of the adsorbate-Au interaction.

Furthermore, the lower partial negative charge upon gold incorporation should decrease the repulsive interaction between adsorbate atoms on the surface. The adsorption energy per adsorbate atom increases with coverage because of the repulsion between partially negative Cl or O atoms. In many cases, the partial charge on the adsorbate is lower when it is incorporated with gold. The decrease in the charge could help drive gold incorporation since in this case the interatomic repulsion of the adsorbate atoms would be lower.

V. CONCLUSIONS

Gold is used in a wide variety of applications making it important to have a complete understanding of the interaction of adsorbates with its surface. We used periodic-slab DFT calculations to investigate the energetics of the morphological changes of the Au(111) surface upon the adsorption of two different electronegative species, chlorine and oxygen. We find that gold adatoms can be pulled out of the surface to become part of the absorbate layer. Generally, the Au-adsorbate interaction is stronger for the incorporated gold surface versus the clean surface. At low coverages this stronger interaction cannot compensate for the cost of creating the adatoms on the surface. As the coverage of the adsorbate increases, a transition occurs where the cost for creating adatoms is compensated and the adsorbate system containing incorporated gold atoms becomes lower in energy. Along with these morphological changes, the nature of the Au-adsorbate interaction changes as a function of coverage and gold incorporation. The Au-adsorbate bonding becomes more covalent with higher coverage or upon the incorporation of gold adatoms, resulting in a smaller adsorbate partial charge with more electron density located directly between the adsorbate and Au. The trends found in this work are qualitatively similar for the adsorption of chlorine and oxygen, but chlorine prefers coordination to fewer surface gold atoms than oxygen; upon adatom incorporation the chlorine is only coordinated to a single gold adatom while oxygen can coordinate with the gold adatom and gold atoms in the top complete layer of gold. Our results are useful in understanding the interaction of chlorine and oxygen with gold, especially in systems where the surface morphology or electronic nature of the surface plays an important role.

ACKOWLEDGEMENTS

This work was supported in part by a graduate school fellowship from the National Science Foundation and the Harvard MRSEC which is funded by NSF under Grant No. DMR-02-13805 and NSEC under Grant No. PHY-06-46094. The authors would like to thank NNIN, a facility funded by NSF, and the CyberInfrastructure Laboratory of the School of Engineering and Applied Sciences at Harvard University for computational resources.

[1] K. W. Kolasinski, *Surface Science: Foundations of Catalysis and Nanoscience* (Wiley, New York, 2008).
[2] P. E. Laibinis, G. M. Whitesides, D. L. Allara, Y. Tao, A. N. Parikh, and R. G. Nuzzo, J. Am. Chem. Soc. **113**, 7152 (1991).
[3] A. Ulman, Chem. Rev. (Washington, D.C.) **96**, 1533 (1996).
[4] A. Kumar, H. A. Biebuyck, and G. M. Whitesides, Langmuir **10**, 1498 (1994).
[5] C. M. Fischer, M. Burghard, S. Rith, and K. V. Klitzing, Appl. Phys. Lett. **66**, 3331 (1995).
[6] A. V. Ellis, K. Vijayamohanan, R. Goswami, N. Chakrapani, L. S. Ramanathan, P. M. Ajayan, and G. Ramanath, Nano Lett. **3**, 279 (2003).
[7] B. Ozturk, C. Blackledge, B. N. Flanders, and D. R. Grischkowsky, Appl. Phys. Lett. **88**, 073108 (2006).
[8] J. Janata and M. Josowicz, Nature Mater. **2**, 19 (2003).
[9] J. Liu and Y. Lu, J. Am. Chem. Soc. **125**, 6642 (2003).
[10] Z. Siwy, L. Trofin, P. Kohli, L. A. Baker, C. Trautmann, and C. R. Martin, J. Am. Chem. Soc. **127**, 5000 (2005).
[11] E. Ozbay, Science **311**, 189 (2006).
[12] J. Biener, G. W. Nyce, A. M. Hodge, M. M. Biener, A. V. Hamza, and S. A. Maier, Adv. Mater. (Weinheim, Ger.) **20**, 1211 (2008).
[13] M. Valden, X. Lai, and D. W. Goodman, Science **281**, 1647 (1998).
[14] M. Valden, S. Pak, X. Lai, and D. W. Goodman, Catal. Lett. **56**, 7 (1998).
[15] M. Comotti, W. C. Li, B. Spliethoff, and F. Schuth, J. Am. Chem. Soc. **128**, 917 (2006).
[16] N. Lopez, T. V. W. Janssens, B. S. Clausen, Y. Xu, M. Mavrikakis, T. Bligaard, and J. K. Norskov, J. Catal. **223**, 232 (2004).
[17] S. M. Driver, T. F. Zhang, and D. A. King, Angew. Chem., Int. Ed. **46**, 700 (2007).
[18] S. Y. Quek, M. M. Biener, J. Biener, J. Bhattacharjee, C. M. Friend, U. V. Waghmare, and E. Kaxiras, J. Phys. Chem. B **110**, 15663 (2006).
[19] P. Maksymovych, D. C. Sorescu, D. Dougherty, and J. T. Yates, J. Phys. Chem. B **109**, 22463 (2005).
[20] L. M. Molina and B. Hammer, Chem. Phys. Lett. **360**, 264 (2002).
[21] S. Narasimhan and D. Vanderbilt, Phys. Rev. Lett. **69**, 1564 (1992).
[22] C. E. Bach, M. Giesen, H. Ibach, and T. L. Einstein, Phys. Rev. Lett. **78**, 4225 (1997).
[23] H. Ibach, J. Vac. Sci. Technol. A **12**, 2240 (1994).
[24] M. M. Biener, J. Biener, and C. M. Friend, Langmuir **21**, 1668 (2005).
[25] H. Ibach, C. E. Bach, M. Giesen, and A. Grossmann, Surf. Sci. **375**, 107 (1997).
[26] D. Sander, U. Linke, and H. Ibach, Surf. Sci. **272**, 318 (1992).
[27] B. K. Min, X. Deng, D. Pinnaduwage, R. Schalek, and C. M. Friend, Phys. Rev. B **72**, 121410 (2005).
[28] J. Biener, M. M. Biener, T. Nowitzki, A. V. Hamza, C. M. Friend, V. Zielasek, and M. Baumer, ChemPhysChem **7**, 1906 (2006).
[29] B. K. Min, A. R. Alemozafar, D. Pinnaduwage, X. Deng, and C. M. Friend, J. Phys. Chem. B **110**, 19833 (2006).
[30] N. D. Spencer and R. M. Lambert, Surf. Sci. **107**, 237 (1981).
[31] G. N. Kastanas and B. E. Koel, Appl. Surf. Sci. **64**, 235 (1993).
[32] W. W. Gao, T. A. Baker, L. Zhou, D. S. Pinnaduwage, E. Kaxiras, and C. M. Friend, J. Am. Chem. Soc. **130**, 3560 (2008).
[33] G. Kresse and J. Hafner, Phys. Rev. B **47**, 558 (1993).
[34] J. P. Perdew and Y. Wang, Phys. Rev. B **45**, 13244 (1992).
[35] D. Vanderbilt, Phys. Rev. B **41**, 7892 (1990).
[36] G. Kresse and J. Hafner, J. Phys.: Condens. Matter **6**, 8245 (1994).
[37] C. Kittel, *Introduction to Solid State Physics* (Wiley, New York, 1996).
[38] F. R. Boer, R. Boom, W. C. M. Mattens, A. R. Miedema, and A. K. Niessen, *Cohesion in Metal* (North-Holland, Amsterdam, 1988).
[39] R. F. W. Bader, *Atoms in Molecules: A Quantum Theory* (Oxford Science, Oxford, 1990).
[40] G. Henkelman, A. Arnaldsson, and H. Jonsson, Comput. Mater. Sci. **36**, 354 (2006).
[41] K. P. H. Huber, *Molecular Spectra and Molecular Structure Constant of Diatomic Molecules* (Van Nostrand, New York, 1979).
[42] B. Hammer, L. B. Hansen, and J. K. Norskov, Phys. Rev. B **59**, 7413 (1999).
[43] P. Broqvist, L. M. Molina, H. Gronbeck, and B. Hammer, J. Catal. **227**, 217 (2004).
[44] M. Mavrikakis, P. Stoltze, and J. K. Norskov, Catal. Lett. **64**, 101 (2000).
[45] M. Gajdos, J. Hafner, and A. Eichler, J. Phys.: Condens. Matter **18**, 13 (2006).
[46] J. Wang, M. R. Voss, H. Busse, and B. E. Koel, J. Phys. Chem. B **102**, 4693 (1998).
[47] J. M. Gottfried, N. Elghobashi, S. L. M. Schroeder, and K. Christmann, Surf. Sci. **523**, 89 (2003).
[48] M. M. Biener, J. Biener, and C. M. Friend, Surf. Sci. **590**, L259 (2005).
[49] N. D. S. Canning, D. Outka, and R. J. Madix, Surf. Sci. **141**, 240 (1984).
[50] N. Saliba, D. H. Parker, and B. E. Koel, Surf. Sci. **410**, 270 (1998).
[51] E. Kaxiras, Y. Baryam, J. D. Joannopoulos, and K. C. Pandey, Phys. Rev. B **35**, 9625 (1987).
[52] G. X. Qian, R. M. Martin, and D. J. Chadi, Phys. Rev. B **38**, 7649 (1988).
[53] K. Reuter and M. Scheffler, Phys. Rev. B **68**, 045407 (2003).
[54] K. Reuter and M. Scheffler, Phys. Rev. B **65**, 035406 (2001).
[55] J. L. Gole and R. N. Zare, J. Chem. Phys. **57**, 5331 (1972).
[56] H. Shi and C. Stampfl, Phys. Rev. B **76**, 075327 (2007).
[57] B. Hammer and J. K. Norskov, *Advances in Catalysis* (Elsevier, New York, 2000), Vol. 45, p. 71.
[58] R. Hoffmann, Rev. Mod. Phys. **60**, 601 (1988).
[59] T. A. Baker, C. M. Friend, and E. Kaxiras, J. Am. Chem. Soc. **130**, 3720 (2008).